Computers and Structures 88 (2010) 87–94

Contents lists available at ScienceDirect

Computers and Structures

journal homepage: www.elsevier.com/locate/compstruc

A finite element procedure for multiscale wave equations with application to plasma waves

Haruhiko Kohno [a,*], Klaus-Jürgen Bathe [b], John C. Wright [a]

[a] Plasma Science and Fusion Center, Massachusetts Institute of Technology, 77 Massachusetts Avenue, Cambridge, MA 02139-4307, USA
[b] Department of Mechanical Engineering, Massachusetts Institute of Technology, Cambridge, MA, USA

ARTICLE INFO

Article history:
Received 8 April 2009
Accepted 1 May 2009
Available online 2 June 2009

Keywords:
Waves
Multi-scale
Spectral method
Finite elements
Plasma
Radio frequencies

ABSTRACT

A finite element wave-packet procedure is presented to solve problems of wave propagation in multi-scale behavior. The proposed scheme combines the advantages of the finite element and spectral methods. The basic formulation is presented, and the capabilities of the procedure are demonstrated through the solution of some illustrative problems, including a problem that characterizes the mode-conversion behavior in plasmas.

1. Introduction

Although much research effort has been spent on solving wave propagation problems, the accurate solution of many such problems is frequently still difficult, in particular when multi-scale behavior is involved. Of course, in general, a numerical solution needs to be employed [1,2]. However, when wave numbers vary in magnitude over the domain, the wave numbers may be very large in certain regions, in particular where there is resonance, requiring a fine mesh to capture this fine-scale variation accurately. In this case, if conventional numerical methods are used, even though most of the domain should not require a fine mesh, we still have to provide the fine discretization for the entire domain. The reason is that the waves will travel throughout the domain and we cannot predict precisely prior to the analysis where resonance will occur. Indeed, frequently, it is the objective of the analysis to detect the regions of resonance.

A specific example in mind is the solution of waves in plasmas. Applying radio-frequency waves in order to raise plasma temperatures is an important subject of research for nuclear fusion. Much effort has been directed to uncover the mechanisms of electromagnetic wave propagations in plasmas (see Refs. [3,4] and the references therein) and computer programs to solve wave propagations in plasmas have been developed [5–7]. Since in these numerical solutions also the phenomenon of mode conversion needs to be addressed, the usual numerical techniques to solve wave propagation problems are not efficient.

To solve wave propagation problems accurately, the spectral method [8] or spectral finite element method have been used [9–11] and good results have been obtained in certain analyses. However, these methods can be computationally expensive, and more importantly, the methods show intrinsic difficulties in satisfying the boundary conditions for arbitrary-shaped domains. Since in many wave propagation analyses, the domain considered is geometrically complex, the available spectral techniques may not be effective.

Another possibly more efficient approach is to utilize basic interpolation functions that are enriched with waves. This means in essence to construct special interpolation functions that are more amenable to capture the desired response. This approach is rather natural to increase the effectiveness of the finite element method for the solution of specific problems, and has been pursued for a long time, like for example (that is, not giving an exhaustive list of references) in the analysis of wave propagations [12–14], global local solutions [15,16], piping analyses [17], the development of beam elements [18], and in fluid flow analyses [19,20]. Such methods have lately also been referred to as partition of unity methods or extended finite element methods, see for example [21–24]. In addition, recently, discontinuous Galerkin methods [25] and related techniques have been researched for the solution of wave propagation problems, but these techniques are computationally very expensive to use.

* Corresponding author.
E-mail address: kono@mit.edu (H. Kohno).

0045-7949/$ - see front matter © 2009 Elsevier Ltd. All rights reserved.
doi:10.1016/j.compstruc.2009.05.001

Whenever such a problem-specific method is proposed, the generality for a specific class of problems and effectiveness are crucial. For plasma wave problem solutions, Pletzer et al. proposed a wave-packet approach using the Gabor functions as envelopes [26]. Although this method has several good features, five parameters need to be selected, where it is difficult to find near optimal choices. Also, since the values of the Gabor functions are nonzero in the entire calculation domain, a cutoff value has to be defined. Furthermore, it is difficult to incorporate general boundary conditions.

Our objective in this paper is to present a finite element scheme in which basic finite element interpolations are used enriched with wave packets. The method is quite simple and is based on the standard finite element method [1] and spectral method [8], but does not have the above-mentioned disadvantages. It turns out that the resulting interpolation functions have the same structure as those proposed in References [12,13] but can be applied to a much broader range of problems. Specifically, the procedure can also be used to solve a range of plasma wave propagation problems, for example in which mode conversion occurs. In these cases, waves with dramatically different wavelengths can exist in localized regions, which are determined by sophisticated plasma models considering kinetic effects. An important point is that the governing equations corresponding to the kinetic models include integrals, since the dielectric tensor is evaluated by integrating over the whole of velocity space and past particle trajectory time. For that reason, the methods referenced above [12–14,21,22] cannot directly be used to solve such plasma wave problems, because they use solutions of some specific differential equations. Our approach utilizes classical finite element interpolations with spectral enrichments, and can be applied to the equations including integrals as well as general differential equations. The combined interpolation technique can be used to easily satisfy Dirichlet boundary conditions and solve for many different wave numbers in one solution.

We first present the numerical procedure in detail and then give the solutions of some test problems, including a problem modelling wave behavior in plasmas. We show that the proposed finite element method gives more accurate results than the conventional finite element method for wave propagation problems. While we only consider one-dimensional linear problems, there is considerable intrinsic potential of the method to be effective for multi-dimensional and even nonlinear solutions.

2. Finite element wave-packet approach

The method proposed here is based on three important features: the technique can be thought of as using the interpolations of the traditional finite element method enriched by waves, the resultant global coefficient matrix is sparse as in finite element methods, and the boundary conditions are easily incorporated. The purpose of this section is to describe each feature in detail.

2.1. Foundation of the numerical method

The basis of the proposed scheme is a weak form of the weighted residual method [1]. Consider a general one-dimensional ordinary differential equation written as $L[u] + f(x) = 0$, where L is an ordinary differential operator. Let $\hat{u}$ be an approximate numerical solution. The numerical solution $\hat{u}$ is determined such that the following integral equation is satisfied:

$$\int_{\Omega} h(x)(L[\hat{u}] + f(x))d\Omega + \int_{\Gamma} h(x)(B[u] - B[\hat{u}])d\Gamma = 0, \tag{1}$$

where $h(x)$ is a weight function, B is an operator for the boundary term, Ω and Γ denote the calculation domain and its boundary, respectively. Using the standard Galerkin approach, the numerical solution and the weight function are given by the same type of interpolation functions, which are formulated next.

2.2. Linear, quadratic and Hermitian wave-packet interpolation functions

The interpolation functions are constructed by multiplying sinusoidal functions by well-known finite element interpolation functions. First, the numerical solution $\hat{u}$ and the weight function h are expressed using the linear or quadratic wave-packet interpolation functions $g_{(i,j)}$ as follows:

$$\hat{u}(x) = g_{(i,j)}(x)u_{(i,j)}, \quad h(x) = g^{*}_{(i',j')}(x)h_{(i',j')}, \tag{2}$$

where the superscript * denotes the complex conjugate; $u_{(i,j)}$, $h_{(i',j')}$ are nodal complex variables in the coordinate-frequency space identified by the global node number i (i') and the harmonic number j (j'). Here the summation convention applies to the subscripts i and j. Since our methods utilize a finite element interpolation function as an envelope function, the value of the envelope function is one at some nodal point x_k and zero at every x_j ($j \neq k$). This allows the functions $g_{(i,j)}$ to be defined locally as follows.
For the linear case:

$$g_{(\alpha,j)}(\xi) = \frac{1}{2}(1 + \xi_\alpha \xi)\exp\left[i2\pi\nu_j\left(x_e + \frac{\Delta x}{2}\xi\right)\right]. \tag{3}$$

For the quadratic case:

$$g_{(\alpha,j)}(\xi) = \left[\frac{\xi_\alpha \xi}{2}(1 + \xi_\alpha \xi) + (1 - \xi_\alpha^2)(1 - \xi^2)\right]\exp\left[i2\pi\nu_j\left(x_e + \frac{\Delta x}{2}\xi\right)\right], \tag{4}$$

where i, x_e, Δx and ξ are the imaginary unit, the x-coordinate at the center of an element, the length of an element and the coordinate variable in the calculation space ($-1 \leqslant \xi \leqslant 1$), respectively; the physical space is then related to the calculation space by $x = x_e + (\Delta x/2)\xi$. The subscript α denotes the local node number, and the values of ξ_α are $\xi_{1,2} = -1$, 1 for the linear case and $\xi_{1,2,3} = -1$, 1, 0 for the quadratic case, respectively. The wave numbers $2\pi\nu_j$ are determined by $\nu_j = j\nu$, where ν is the fundamental frequency and j is an integer in the range $-(N_F - 1)/2 \leqslant j \leqslant (N_F - 1)/2$ with the cutoff number of harmonics N_F. Here $N_F \geqslant 1$ is an odd integer. The schematic profile of a linear wave-packet interpolation function is shown in Fig. 1. As we will see in numerical examples in Section 4, the quadratic wave-packet interpolation is actually more effective.

Another possibly more efficient wave-packet approach can be established by employing Hermitian cubic beam functions [1] where then the nodal values and also the derivative values at the nodes are used. This makes the expressions for the numerical solution and the weight function slightly different from Eq. (2):

$$\hat{u}(x) = g_{(i,j)}(x)\tilde{u}_{(i,j)}, \quad h(x) = g^{*}_{(i',j')}(x)\tilde{h}_{(i',j')}. \tag{5}$$

Here the Hermitian wave-packet interpolation functions comprise two different expressions:

$$\begin{aligned} g_{(i,j)} &= g^1_{(i,j)} \quad \tilde{u}_{(i,j)} = u_{(i,j)} \quad \text{for } 1 \leqslant i \leqslant N_x, \\ &= g^2_{(k,j)}, \qquad\quad = u'_{(k,j)} \quad \text{for } N_x + 1 \leqslant i \leqslant 2N_x \end{aligned} \tag{6}$$

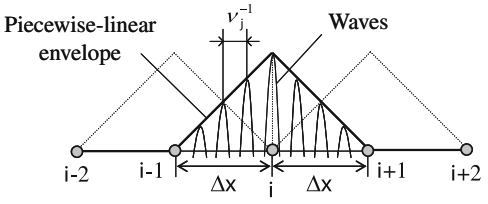

Fig. 1. Schematic diagram of a linear wave-packet interpolation function.

(same applies to $\tilde{h}_{(i,j)}$), where N_x is the total number of nodes, and the value of the subscript k is related to the value of i by $k = i - N_x$. In a similar way to the linear and quadratic wave-packet interpolations, these functions in Eq. (6) can be written locally as follows:

$$g^1_{(\alpha,j)}(\xi) = \frac{1}{4}(\xi+\xi_\alpha)^2(-\xi_\alpha\xi+2)\exp\left[i2\pi v_j\left(x_e+\frac{\Delta x}{2}\xi\right)\right],$$
$$g^2_{(\alpha,j)}(\xi) = \frac{\Delta x}{8}(\xi+\xi_\alpha)^2(\xi-\xi_\alpha)\exp\left[i2\pi v_j\left(x_e+\frac{\Delta x}{2}\xi\right)\right], \quad (7)$$

where $\xi_{1,2} = -1, 1$. The real-valued profiles of the Hermitian wave-packet interpolation functions are shown in Fig. 2.

For a real-valued solution, we can easily derive the following restrictions from Eqs. (2) and (5):

$$u_{(\alpha,j)} = u^*_{(\alpha,-j)}, u'_{(\alpha,j)} = u'^*_{(\alpha,-j)}, \quad (8)$$

where the equation involving derivatives is of course only considered for the Hermitian wave-packet interpolation functions. These relations reduce the number of unknowns to half and consequently, the size of the global matrix to a quarter. Using Eq. (8), for example, we can modify the linear wave-packet interpolation functions as follows:

$$\hat{u}(x) = g^a_{(\alpha,0)}u_{(\alpha,0)} + \sum_{j=1}^{(N_F-1)/2}\left[g^b_{(\alpha,j)}u^{(R)}_{(\alpha,j)} + g^c_{(\alpha,j)}u^{(I)}_{(\alpha,j)}\right] = g_{(\alpha,m)}\tilde{u}_{(\alpha,m)}, \quad (9)$$

with

$$g^a_{(\alpha,0)} = \frac{1}{2}(1+\xi_\alpha\xi),$$
$$g^b_{(\alpha,j)} = (1+\xi_\alpha\xi)\cos\left[2\pi v_j\left(x_e+\frac{\Delta x}{2}\xi\right)\right], \quad (10)$$
$$g^c_{(\alpha,j)} = -(1+\xi_\alpha\xi)\sin\left[2\pi v_j\left(x_e+\frac{\Delta x}{2}\xi\right)\right]$$

$$\begin{aligned} g_{(\alpha,m)} &= g^a_{(\alpha,0)} \quad \tilde{u}_{(\alpha,m)} = u_{(\alpha,0)} \quad \text{for } m = 0,\\ &= g^b_{(\alpha,j)}, \qquad = u^{(R)}_{(\alpha,j)} \quad \text{for } 1 \leqslant m \leqslant (N_F-1)/2,\\ &= g^c_{(\alpha,k)} \qquad = u^{(I)}_{(\alpha,k)} \quad \text{for } (N_F-1)/2+1 \leqslant m \leqslant N_F-1, \end{aligned} \quad (11)$$

where $u^{(R)}_{(\alpha,j)}$, $u^{(I)}_{(\alpha,j)}$ are the real and imaginary parts of $u_{(\alpha,j)}$, respectively, and the subscripts j, k and m in Eq. (11) are related to one another by $j = m$, $k = m - (N_F - 1)/2$. Of course, if we consider a general plasma wave, the numerical solution is always complex, and hence Eqs. (8)–(11) are not applicable.

An interesting observation is that for $j = 0$ all the wave-packet interpolation functions given in Eqs. (3), (4), and (7) reduce to the usual finite element interpolation functions as a result of $v_j = jv = 0$. Thus, for $N_F = 1$, the present interpolation scheme consists only of the conventional finite element interpolation functions, and indeed the present wave-packet approach is identical to the conventional finite element method when $N_F = 1$ (see Section 2.3). We will see that this property leads to the straightforward treatment of the boundary conditions.

The present scheme results in a relatively low computational cost since the global matrix is sparse. This sparsity is due to the local interpolation of wave packets. As an example, we show the distribution of the global matrix elements for the case of using the Hermitian functions in Fig. 3, where the nonzero regions are block-diagonalized with a regular bandwidth of $3N_F$.

As an illustration, consider a one-dimensional sine-wave problem described by $u'' + \alpha^2 u = 0$ in the range $0 \leqslant x \leqslant 1$ subject to the boundary conditions $u(0) = 0$, $u'(1) = \alpha$. Here α is a constant with $\cos\alpha = 1$. The exact solution for this problem is then given by $u = \sin(\alpha x)$. Fig. 4a shows a numerical solution obtained by the linear finite element wave-packet approach for $\alpha = 4\pi$, $v = 0.5$, $N_x = 2$ and $N_F = 9$. As seen, with only one element used, we obtain virtually the exact analytical results. This is the desired result since the method is based on the Fourier decomposition technique so that any smooth function should be reproduced by the combination of sinusoidal waves with different wave numbers regardless of the value of N_x. Fig. 4b is a semi-log plot of the error norm, which is defined by $\|\cdot\| \equiv [\int(u-\hat{u})^2dx/\int u^2dx]^{1/2}$, as a function of N_F. We notice that the error decreases logarithmically with the number of harmonics for $N_F \geqslant 5$. Due to this feature, the present wave-packet approach can yield more accurate results compared to the conventional finite element method by orders of magnitude.

2.3. Imposing the boundary conditions

An important feature of the present method is the ease of imposing the boundary conditions. Consider a one-dimensional problem governed by a second-order differential equation. When imposing the Dirichlet boundary condition, we choose a weight function whose value is forced to be zero at the boundary in the

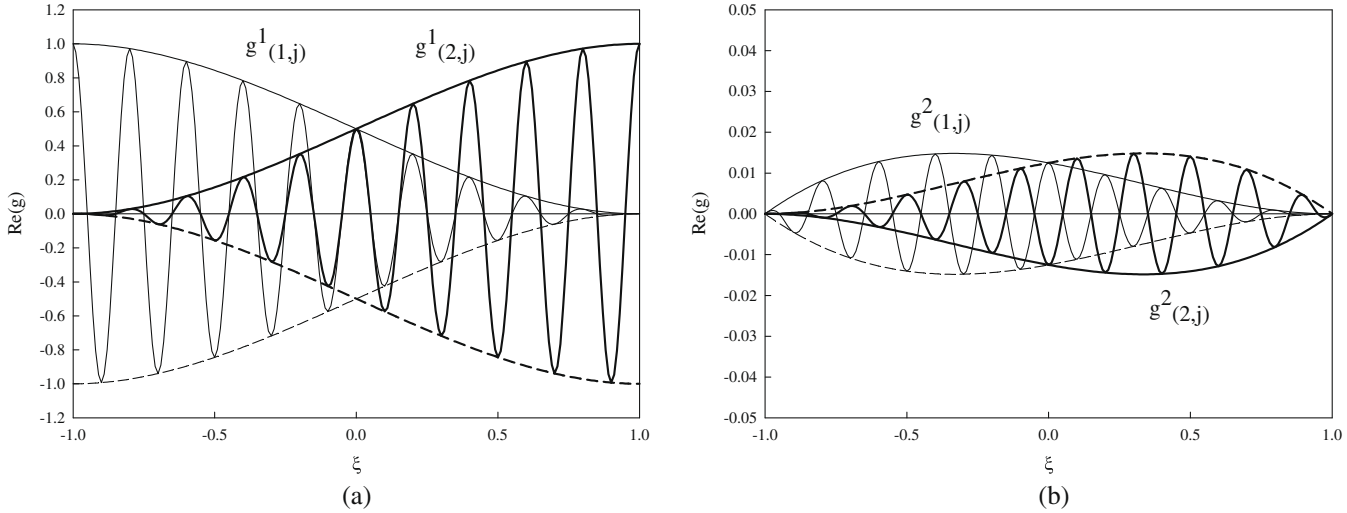

Fig. 2. Profiles of the Hermitian wave-packet interpolation functions together with their envelope functions for $\Delta x = 0.1$ and $v_j = 100$: (a) plot of $\mathrm{Re}[g^1_{(\alpha,j)}]$ vs. ξ; and (b) plot of $\mathrm{Re}[g^2_{(\alpha,j)}]$ vs. ξ.

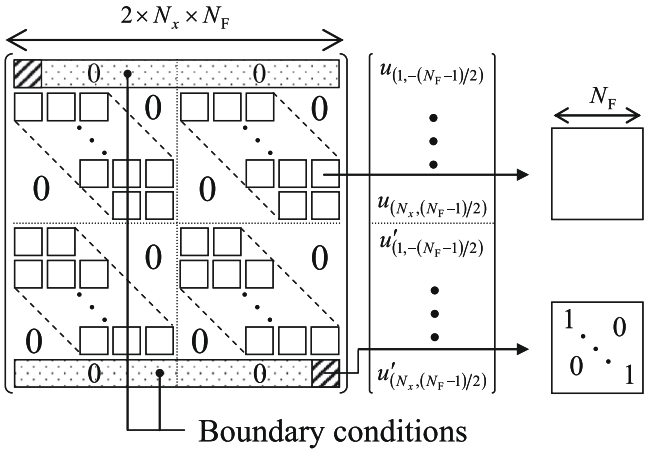

Fig. 3. An example of the structure of the global matrix for the analysis using the Hermitian finite element wave-packet method.

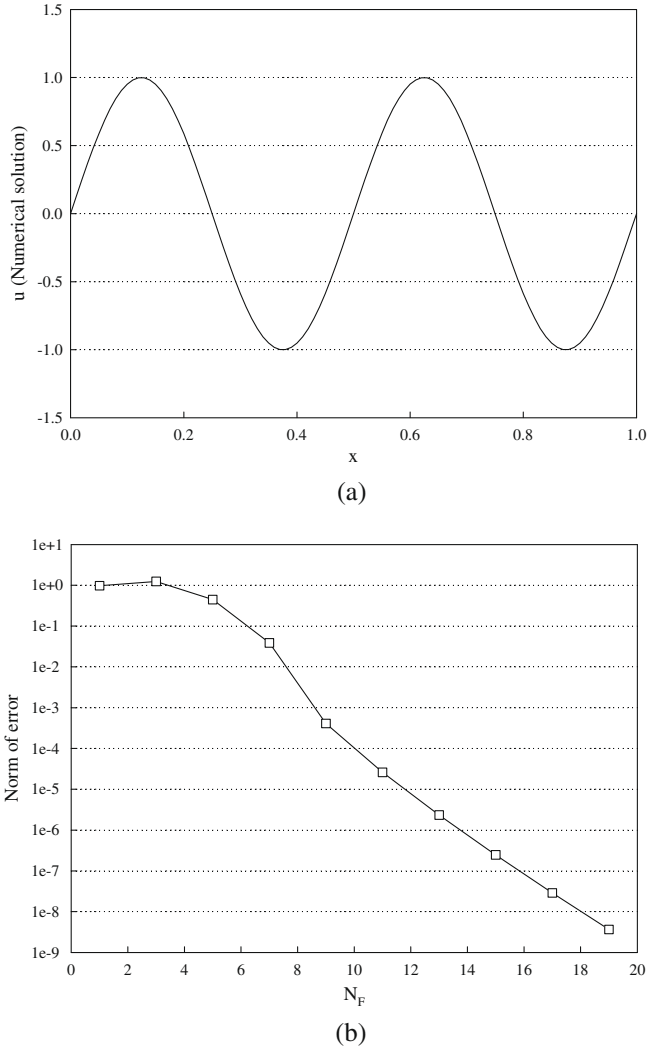

Fig. 4. The numerical results obtained by the linear finite element wave-packet method for $v = 0.5$, $N_x = 2$: (a) the calculated wave for $N_F = 9$; (b) the norm of error as a function of N_F.

same way as in the conventional Galerkin finite element methods. But an important point to notice is that the interpolated nodal values $u_{(i,j)}$ (or $\tilde{u}_{(i,j)}$) are not identical to the nodal values of the numerical solution $\hat{u}(x)$. Thus, for example, if we intend to exactly satisfy the Dirichlet boundary condition at the boundary $x = x_b$ (the right-hand side boundary), the following equality must be satisfied:

$$\begin{aligned}&\hat{u}(x_b) = g_{(i,j)}(x_b)u_{(i,j)} = u_b \quad \text{(for the linear/quadratic case)},\\ &\hat{u}(x_b) = g_{(i,j)}(x_b)\tilde{u}_{(i,j)} = u_b \quad \text{(for the Hermitian case)}\end{aligned} \tag{12}$$

For u_b being real, Eq. (12) leads to

$$\begin{cases}\sum_{j=-(N_F-1)/2}^{(N_F-1)/2}\left[\cos(2\pi v_j x_b)u^{(R)}_{(N_x,j)} - \sin(2\pi v_j x_b)u^{(I)}_{(N_x,j)}\right] = u_b,\\ \sum_{j=-(N_F-1)/2}^{(N_F-1)/2}\left[\sin(2\pi v_j x_b)u^{(R)}_{(N_x,j)} + \cos(2\pi v_j x_b)u^{(I)}_{(N_x,j)}\right] = 0,\end{cases} \tag{13}$$

where we note that Eq. (13) does not lead to a unique solution for $N_F > 1$. However, the following choice always satisfies the boundary condition for any v and x_b:

$$\begin{aligned}u^{(R)}_{(N_x,j)} &= u_b \quad \text{for } j = 0,\\ &= 0 \quad \text{for } j \neq 0,\\ u^{(I)}_{(N_x,j)} &= 0 \quad \text{for any } j.\end{aligned} \tag{14}$$

This corresponds to the concept of imposing the exact boundary value in the conventional finite element component ($j = 0$). Note that Eq. (14) is consistent with the statement in Section 2.2; the present scheme reduces to the conventional finite element method for $N_F = 1$.

On the other hand, the proposed method only approximately satisfies the Neumann boundary conditions, again as in the conventional finite element method. For the linear or quadratic wave-packet approach, the value of the weight function at the boundary can be arbitrary. The boundary term in the discretized equation is calculated in the same way as in standard finite element methods. For the Hermitian wave-packet approach, we specify $h'_{(i,j)} = 0$ at the Neumann boundary and choose the boundary nodal values in a similar way to the Dirichlet boundary condition as follows:

$$\begin{aligned}u'^{(R)}_{(N_x,j)} &= u'_b \quad \text{for } j = 0,\\ &= 0 \quad \text{for } j \neq 0,\\ u'^{(I)}_{(N_x,j)} &= 0 \quad \text{for any } j.\end{aligned} \tag{15}$$

Here we assume that the Neumann boundary condition is imposed at $x = x_b$. In general, the above choice does not exactly satisfy the Neumann boundary condition because

$$\begin{aligned}\left.\frac{d\hat{u}}{dx}\right|_{x=x_b} &= \frac{2}{\Delta x}\left(\frac{dg^1_{(\alpha=2,j)}(\xi)}{d\xi}u_{(\alpha=2,j)} + \frac{dg^2_{(\alpha=2,j)}(\xi)}{d\xi}u'_{(\alpha=2,j)}\right)\Bigg|_{\xi=1,x=x_b}\\ &= \frac{2}{\Delta x}\left.\frac{dg^1_{(2,j)}(\xi)}{d\xi}u_{(2,j)}\right|_{\xi=1,x=x_b} + u'_b\end{aligned} \tag{16}$$

In general, the first term on the right-hand side is nonzero so that $d\hat{u}/dx|_{x=x_b} \neq u'_b$. For $N_F = 1$, the scheme reduces to the conventional Hermitian finite element method, and then the Neumann boundary condition is exactly satisfied.

3. A required condition in the fundamental frequency

In the present scheme, we need to specify three numerical parameters: N_x, N_F and v. Here we derive one required condition for a proper choice of v related to the value of N_x.

First of all, an important point is that every integral in the locally discretized equations can be written in the following form:

$$I = \int_{-1}^{1}\left(\sum_{n=0} C_n\xi^n\right)\exp(a\xi + b)d\xi, \tag{17}$$

where

$$a = i\pi(v_j - v_{j'})\Delta x, \quad b = i2\pi(v_j - v_{j'})x_e. \tag{18}$$

Here $n \geqslant 0$ takes integer values, and C_n are the coefficients determined depending on the differential equations considered. Now let

$$F(n) = \int_{-1}^{1} \xi^n \exp(a\xi + b)d\xi. \tag{19}$$

Then Eq. (17) is simply expressed by $I = \sum_{n=0} C_n F(n)$. Consider first the case of $v_j \neq v_{j'}$ (i.e., $j \neq j'$). For $n \geqslant 1$ one can rewrite Eq. (19) as follows:

$$F(n) = \left[\frac{\xi^n}{a}\exp(a\xi + b)\right]_{-1}^{1} - \frac{n}{a}F(n-1). \tag{20}$$

For $n = 0$ we have:

$$F(0) = \int_{-1}^{1} e^{a\xi+b}d\xi = \frac{1}{a}(e^{a+b} - e^{-a+b}). \tag{21}$$

Thus, using Eqs. (20) and (21) we obtain $F(n)$ for any value of n through successive calculations. For $v_j = v_{j'} (j = j')$, the integral in Eq. (19) is easily solved as follows:

$$F(n) = \int_{-1}^{1} \xi^n d\xi = \frac{1}{n+1}[1 - (-1)^{n+1}]. \tag{22}$$

These analytical expressions are desirable since we do not need to apply any numerical integration to the integral shown in Eq. (17); consequently, the computation of each term is fast without a numerical error due to numerical integration.

Now, using Eqs. (20)–(22), consider the following two important limits: $|a| \to \infty$ and $|a| \to 0$. Assume that a given differential equation is discretized by properly choosing finite element wave-packet interpolation functions. For $|a| \to \infty$, we find that $|I_{j=j'}|/|I_{j\neq j'}| \to \infty$ and $|I_{j=j'}| \to \infty$ for $j \neq 0$ in a non-sparse block (i, i'), where $|I_{j=j'}|$ and $|I_{j\neq j'}|$ are the integrals obtained by adding up all the discretized derivative terms for $j = j'$ and $j \neq j'$, respectively, expressed in the form of Eq. (17). On the other hand, for $|a| \to 0$, we find that $|I_{j\neq j'}|/|I_{j=j'}| \to \infty$ and $|I_{j\neq j'}| \to \infty$ in a non-sparse block (i, i'). Of course, the numerical solutions for these cases do not make any sense. Therefore, a required condition should be $|a| \sim 1$, i.e., $v\Delta x \sim 1$, for which the magnitude of every term in Eq. (17) is about like in the conventional finite element discretization ($j = j' = 0$). The physical interpretation of this constraint is that the waves in the wave packet should have at least one wavelength in an element (see Fig. 1).

4. Numerical examples

In this section, we illustrate the performance of the finite element wave-packet approach using three test problems. First, we solve a wave propagation through different media, then we solve the problem described by the Airy-type equation, whose exact solutions are available for comparison with the numerical results. Finally we solve a more difficult problem which models the mode-conversion behavior of the radio-frequency waves in plasmas described by the Wasow equation. We take the last two examples from Ref. [26]. In all solutions we use uniform meshes and when we compare solution accuracies with the accuracy obtained using the conventional finite element method we employ the fact that the solutions are real and use the same number of unknowns (see Section 2.2).

4.1. Wave propagation through different media

Consider the wave propagation problem through different media described by the following equation:

$$\frac{d^2u}{dx^2} + \alpha^2 u = 0, \quad 0 \leqslant x \leqslant 2, \tag{23}$$

where $\alpha^2 = \alpha_I^2$ for $0 \leqslant x < 1$ and $\alpha^2 = \alpha_{II}^2$ for $1 < x \leqslant 2$. We assume that $\sin\alpha_I = \sin\alpha_{II} = 0$ and $\cos\alpha_I = \cos\alpha_{II}$ subject to the boundary conditions $u(0) = 0$ and $u'(2) = \alpha_{II}$. The exact solution is then $u_I = (\alpha_{II}/\alpha_I)\sin(\alpha_I x)$ in the range $0 \leqslant x < 1$ and $u_{II} = \sin(\alpha_{II}x)$ in $1 < x \leqslant 2$. Here we consider two cases: $\alpha_I = 8\pi$, $\alpha_{II} = 4\pi$ in case 1 and $\alpha_I = 64\pi$, $\alpha_{II} = 8\pi$ in case 2.

The discretized equation for Eq. (23) is:

$$\int_{\Omega^e}\left(\frac{dg^*_{(\alpha,j')}}{dx}\frac{dg_{(\beta,j)}}{dx} - \alpha^2 g^*_{(\alpha,j')}g_{(\beta,j)}\right)dx \cdot u_{(\beta j)} - g^*_{(\alpha,j')}\frac{du}{dx}\Big|_{\text{Neumann boundary}} = 0. \tag{24}$$

As for the parameters used in the numerical scheme, we set the number of envelope positions (i.e., nodes), the cutoff number of harmonics and the fundamental frequency to $N_x = 9$, $N_F = 5$, $v = 1.8$ ($N_x = 21$, $N_F = 11$, $v = 6.0$) for the linear, quadratic wave-packet methods and $N_x = 5$, $N_F = 5$, $v = 1.5$ ($N_x = 11$, $N_F = 11$, $v = 6.0$) for the Hermitian wave-packet method in case 1 (case 2).

The profiles of the numerical solutions obtained by the Hermitian wave-packet method are shown in Fig. 5. Fig. 6 shows the

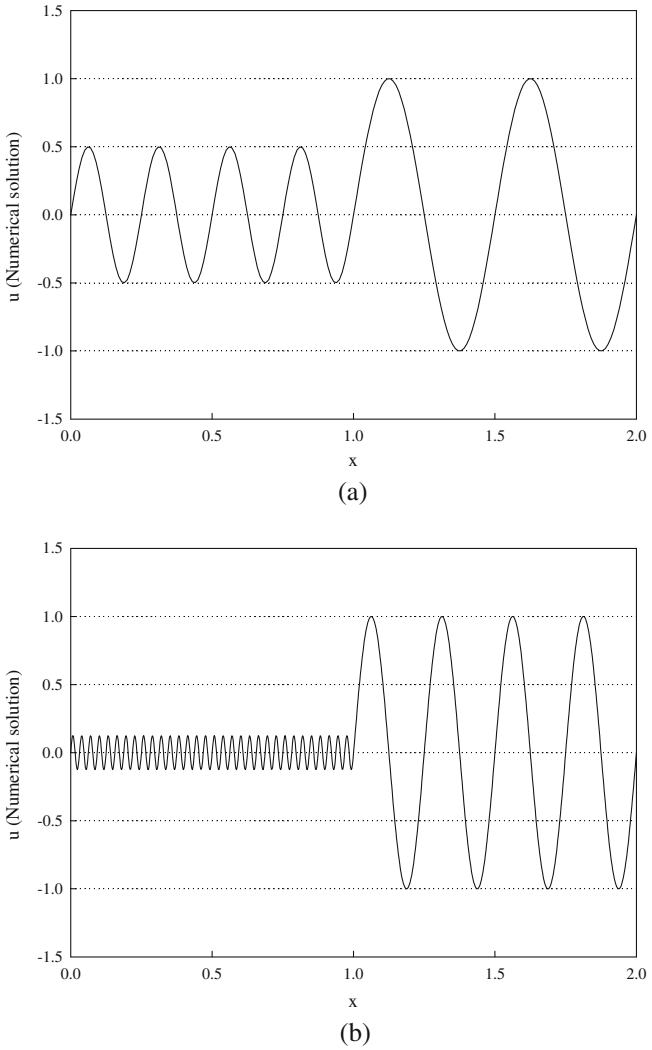

Fig. 5. Numerical solutions of the wave propagation problem through different media: (a) $u = 0.5\sin(8\pi x)$ in $0 \leqslant x < 1$ and $u = \sin(4\pi x)$ in $1 < x \leqslant 2$ (case 1); (b) $u = 0.125\sin(64\pi x)$ in $0 \leqslant x < 1$ and $u = \sin(8\pi x)$ in $1 < x \leqslant 2$ (case 2).

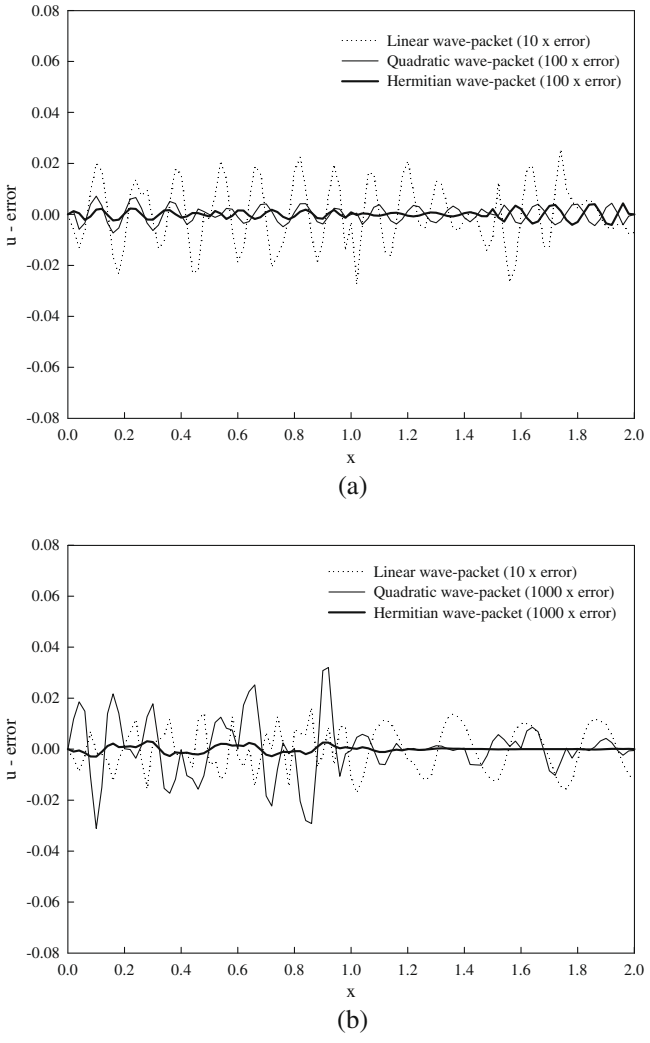

Fig. 6. Comparison of the numerical error for the wave propagation problem through different media among the three different wave-packet methods: (a) case 1; and (b) case 2.

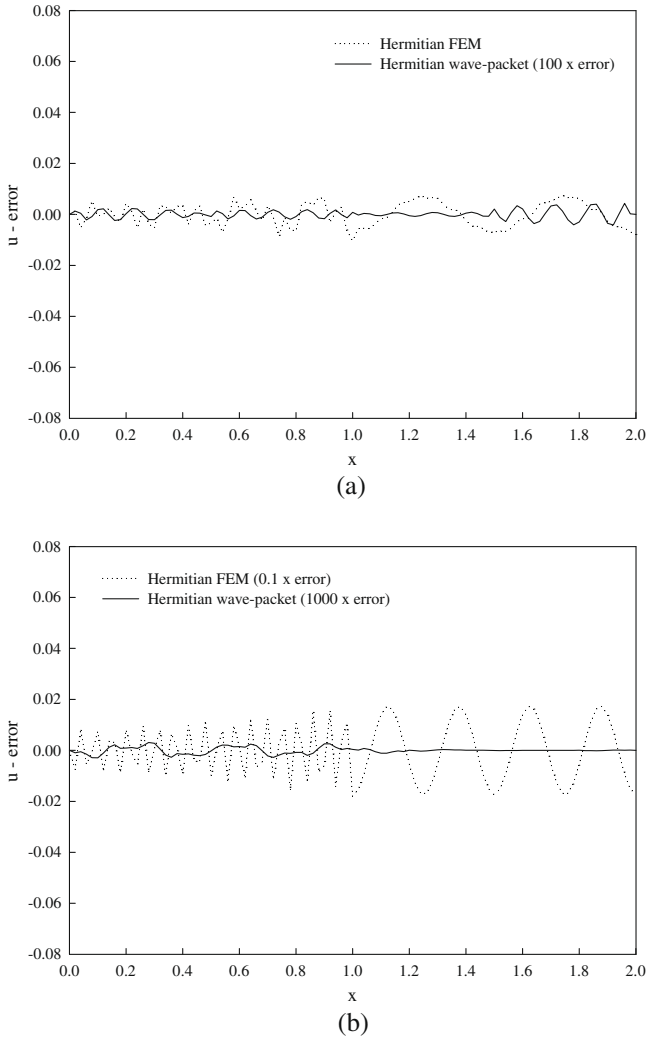

Fig. 7. Comparison of the numerical error for the wave propagation problem through different media between the finite element wave-packet method and the conventional finite element method: (a) case 1; and (b) case 2.

comparison of the numerical error $(\hat{u} - u)$ for the linear, quadratic and Hermitian wave-packet approaches. As seen, the error is considerably smaller if we use higher-order envelope functions, although the difference between the quadratic and Hermitian wave packets is small. Fig. 7 shows the comparison of the numerical error between the present wave-packet method and the conventional finite element method with $N_x = 25$ in case 1 and $N_x = 121$ in case 2, both of which utilize the Hermitian interpolation functions. We see that the numerical results obtained using the Hermitian wave-packet method are several orders of magnitude more accurate than the results obtained using the standard finite element method. Especially, the result in Fig. 7b demonstrates that a sufficient number of harmonics yields rapid convergence for a smooth function as for the standard Fourier series (see Fig. 4b).

4.2. Airy-type equation

Second, the methods are applied to the following second-order differential equation:

$$\frac{d^2u}{dx^2} + \alpha^2(1-2x)u = 0, \quad 0 \leqslant x \leqslant 1, \tag{25}$$

whose exact solution is described by the Airy function: $u = Ai[(\alpha/2)^{2/3}(2x-1)]$. Here the coefficient α is fixed at $21\pi/2$ (the same value as in Ref. [26]), and the corresponding boundary conditions are given by $u'(0) = -8.3239$ and $u'(1) = -9.8696 \times 10^{-5}$. Fig. 8 shows the profile of the corresponding exact solution. The fundamental frequency, the numbers of envelope positions and Fourier modes

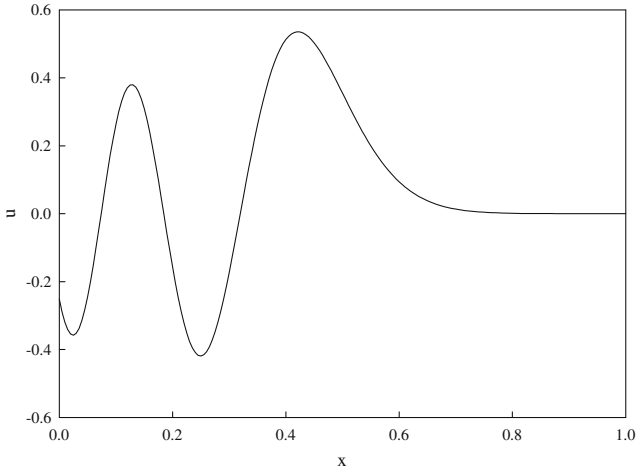

Fig. 8. Exact solution of the Airy-type equation for $\alpha = 21\pi/2$.

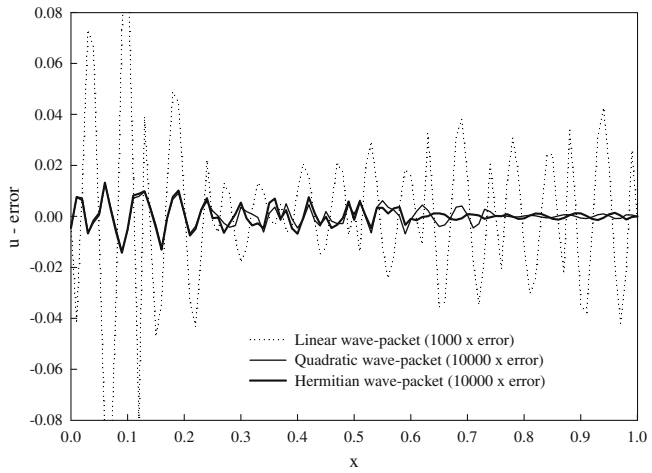

Fig. 9. Comparison of the numerical error for the Airy-type equation among the three different wave-packet methods.

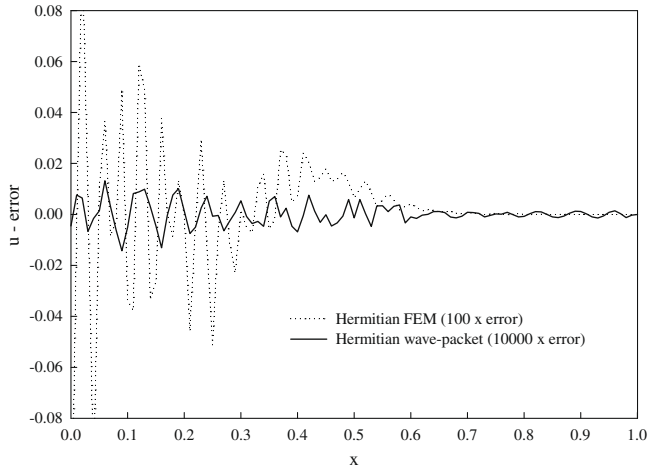

Fig. 10. Comparison of the numerical error for the Airy-type equation between the finite element wave-packet method and the conventional finite element method.

are $v = 2.0$, $N_x = 9$ for the linear, quadratic cases, $N_x = 5$ for the Hermitian case, and $N_F = 5$.

Fig. 9 gives the numerical error for the three different wave-packet approaches. As before, the errors obtained using the higher-order wave-packet interpolations are much smaller than the error obtained using the linear interpolation. Also, it is observed that the higher-order finite element wave-packet methods are comparable in accuracy with the Gabor element method developed by Pletzer et al. [26]. Fig. 10 shows the comparison of the numerical error between the present wave-packet method and the conventional finite element method (with $N_x = 25$), both of which utilize the Hermitian interpolation functions. Again, it is observed that the numerical result using the Hermitian wave-packet method is much more accurate; note that the error-scale differs by two orders of magnitude.

4.3. Wasow equation

Lastly, we consider the numerical solution of the Wasow equation, which models the mode conversion effects of radio-frequency waves in plasmas. The equation considered here is given by

$$\left\{\frac{d^2}{dx^2}+k^2[1-0.5(x-0.5)]\right\}\left\{\frac{d^2}{dx^2}+k^2[1-160(x-0.5)]\right\}u+\alpha u=0,\quad 0\leqslant x\leqslant 1, \tag{26}$$

where $k^2 = 2 \times 10^3$ and $\alpha = 8 \times 10^6$ subject to the boundary conditions $u(0) = 0$, $u(1) = 1$ and $u'(0) = u'(1) = 0$ (the same boundary conditions as in Ref. [26]). Eq. (26) implies the formation of multiscale waves with different wave numbers by a factor of 320. Here a comparison is made between the finite element wave-packet method and the conventional finite element method, both utilizing the Hermitian interpolation functions which can be straightforwardly applied to this fourth-order differential equation. As numerical parameters, we choose $v = 10.5$, $N_x = 10$ and $N_F = 11$.

Since an analytical solution to this problem is not available, we first calculate the problem with a very fine mesh using the Hermitian interpolation functions, and utilize the obtained result as a "quasi-exact" solution. Fig. 11 shows the numerical solution obtained with 1000 elements. We see that the fast and slow waves are coupled on the left half of the domain (see Fig. 11b), while only the slow wave having a shorter wavelength is evanescent on the

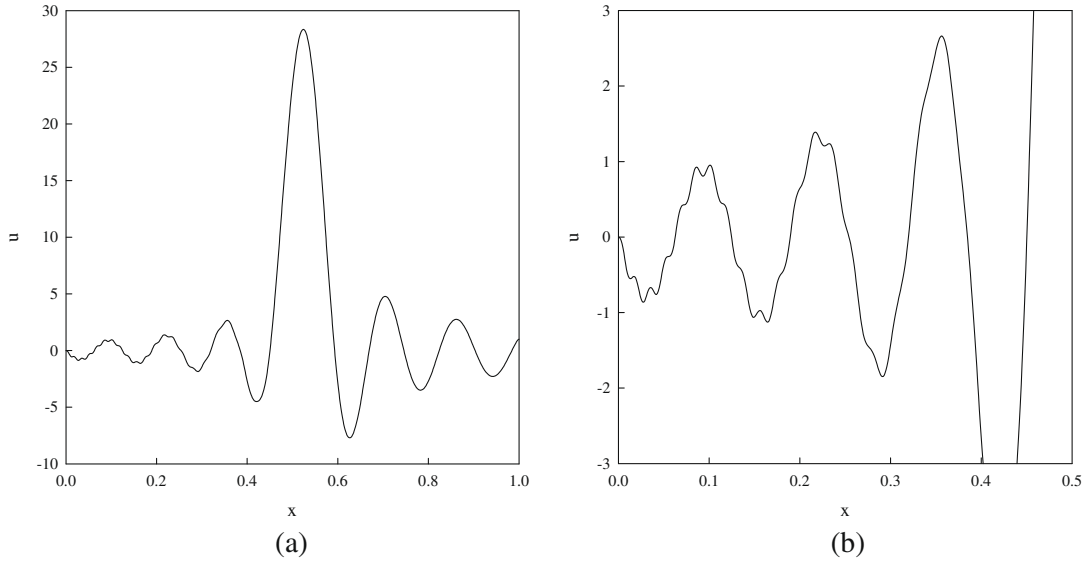

Fig. 11. Numerical solution of the Wasow equation: (a) macroscopic oscillation; and (b) fine scale oscillation.

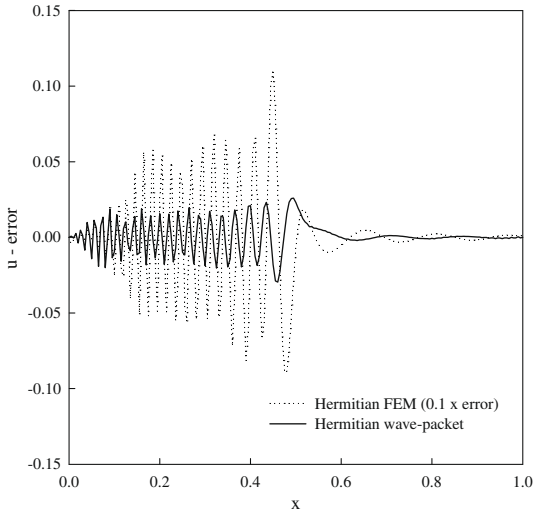

Fig. 12. Comparison of the numerical error for the Wasow equation between the finite element wave-packet method and the conventional finite element method.

right half. This is also confirmed in Eq. (26); although the sign of $r_1 = k^2[1 - 0.5(x - 0.5)]$ is always positive in the entire domain, the sign of $r_2 = k^2[1 - 160(x - 0.5)]$ changes from positive to negative at $x = 0.5$. The former corresponds to propagation of the fast wave at every point, whereas the latter corresponds to evanescence of the slow wave on the right half of the domain. The mixing of these very different waves makes it more difficult to accurately solve the Wasow equation compared to the equations in the previous problems.

A comparison of the numerical error ($\hat{u} - u_{\text{quasi-exact}}$) between the finite element wave-packet method and the conventional finite element method is shown in Fig. 12. Again, the present wave-packet approach gives a more accurate numerical result compared to the conventional finite element solution.

5. Conclusions

We presented in this paper a finite element wave-packet method for the analysis of waves through media, and solved some illustrative problems. The method is in particular directed to solve waves in plasmas accurately with a reasonable computational cost. The key idea is to enrich the usual finite element interpolations with wave packets. We see that this approach results into some favorable features drawing from both, conventional finite element and spectral methods. First, the interpolation functions are locally defined in the same way as in the conventional finite element methods, which is effective for programming. Second, this local definition results in the formation of a sparse global matrix. Third, all the integrals in the discretized equation are analytically solved, yielding simple expressions (of course, numerical integration could be used and probably has to be used for wave equations of higher dimensions). Fourth, the boundary conditions are easily incorporated in the discretized equation. In fact, the Dirichlet and Neumann boundary conditions are treated in a similar way as in the conventional finite element methods. Fifth, using the wave packets can give more accurate results than using the corresponding conventional finite element methods under the same computational costs.

Plasma wave equations can be far more complex than the one-dimensional equations we solved here, but the one-dimensional equations/solutions exhibit some of the fundamental characteristics of these more complex waves. In further research the method should be applied to and tested in two- and three-dimensional solutions with nonuniform meshes. Also, a mathematical convergence analysis should be pursued to identify the rate and order of convergence, and the optimal value of fundamental frequency.

Acknowledgements

We would like to thank Prof. Jeffrey Freidberg and Dr. Paul Bonoli of M.I.T. for their valuable comments on this work for the application to plasmas. This work was supported in part by DoE Contract No. DE-FG02-99ER54525.

References

[1] Bathe KJ. Finite element procedures. Prentice-Hall; 1996.
[2] Cohen GC. Higher-order numerical methods for transient wave equations. Springer; 2001.
[3] Stix TH. Waves in plasmas. American Institute of Physics; 1992.
[4] Freidberg JP. Plasma physics and fusion energy. Cambridge University Press; 2007.
[5] Brambilla M, Krucken T. Numerical simulation of ion cyclotron heating of hot tokamak plasmas. Nucl Fusion 1988;28:1813–33.
[6] Jaeger EF, Berry LA, D'Azevedo E, Batchelor DB, Carter MD. All-orders spectral calculation of radio-frequency heating in two-dimensional toroidal plasmas. Phys Plasmas 2001;8:1573–83.
[7] Wright JC, Bonoli PT, Brambilla M, Meo F, D'Azevedo E, Batchelor DB, et al. Full wave simulations of fast wave mode conversion and lower hybrid wave propagation in tokamaks. Phys Plasmas 2004;11:2473–9.
[8] Karniadakis GE, Sherwin S. Spectral/hp element methods for computational fluid dynamics. 2nd ed. Oxford University Press; 2005.
[9] Gopalakrishnan S, Chakraborty A, Mahapatra DR. Spectral finite element method. Springer-Verlag; 2008.
[10] Beris AN, Armstrong RC, Brown RA. Spectral/finite-element calculations of the flow of a Maxwell fluid between eccentric rotating cylinders. J Non-Newtonian Fluid Mech 1987;22:129–67.
[11] Steppeler J. A Galerkin finite element-spectral weather forecast model in hybrid coordinates. Comput Math Appl 1988;16:23–30.
[12] Astley RJ. Wave envelope and infinite elements for acoustical radiation. Int J Numer Methods Fluids 1983;3:507–26.
[13] Bettess P. A simple wave envelope element example. Commun Appl Numer Methods 1987;3:77–80.
[14] Bettess P, Chadwick E. Wave envelope examples for progressive waves. Int J Numer Methods Eng 1995;38:2487–508.
[15] Avanessian V, Dong SB, Muki R. Forced asymmetric vibrations of an axisymmetric body in contact with an elastic half-space – a global–local finite element approach. J Sound Vib 1987;114:45–56.
[16] Belytschko T, Lu YY. Global-local finite element-spectral-boundary element techniques for failure analysis. Comput Struct 1990;37:133–40.
[17] Bathe KJ, Almeida C. A simple and effective pipe elbow element – linear analysis. J Appl Mech 1980;47:93–100.
[18] Dvorkin EN, Celentano D, Cuitino A, Gioia G. A Vlasov beam element. Comput Struct 1989;33:187–96.
[19] Kohno H, Bathe KJ. A flow-condition-based interpolation finite element procedure for triangular grids. Int J Numer Methods Fluids 2006;51:673–99.
[20] Banijamali B, Bathe KJ. The CIP method embedded in finite element discretizations of incompressible flows. Int J Numer Methods Eng 2007;71:66–80.
[21] Melenk JM, Babuška I. The partition of unity finite element method: basic theory and applications. Comput Methods Appl Mech Eng 1996;139:289–314.
[22] Babuška I, Melenk JM. The partition of unity method. Int J Numer Methods Eng 1997;40:727–58.
[23] Sukumar N, Moes N, Moran B, Belytschko T. Extended finite element method for three-dimensional crack modelling. Int J Numer Methods Eng 2000;48:1549–70.
[24] Fries TP, Belytschko T. The intrinsic XFEM: a method for arbitrary discontinuities without additional unknowns. Int J Numer Methods Eng 2006;68:1358–85.
[25] Bathe KJ, editor. Computational fluid and solid mechanics. Proceedings of the third MIT conference on computational fluid and solid mechanics 2005. Amsterdam: Elsevier; 2005.
[26] Pletzer A, Phillips CK, Smithe DN. Gabor wave packet method to solve plasma wave equations. Proceedings of the 15th topical conference on radio frequency power in plasmas, vol. 694; 2003. p. 503–6.